JOC The Journal of Organic Chemistry

Article

pubs.acs.org/joc

Electronic vs Steric Effects on the Stability of Anionic Species: A Case Study on the Ortho and Para Regioisomers of Organofullerenes

Wei-Wei Chang, Zong-Jun Li, Fa-Gui He, Tao Sun, and Xiang Gao*

State Key Laboratory of Electroanalytical Chemistry, Changchun Institute of Applied Chemistry, University of the Chinese Academy of Sciences, Chinese Academy of Sciences, 5625 Renmin Street, Changchun 130022, Jilin, China

Supporting Information

ABSTRACT: The stability of the anionic species of the ortho and para regioisomers of (MeO)BnC_{2n} (Me = methyl, Bn = benzyl, n = 30 or 35) has been examined. The results show that the ortho adducts (electronically favored regioisomers) are stable upon receiving one or two electrons, while the para ones (sterically favored adducts) decompose by removing the methoxy group under similar conditions. Computational calculations indicate that the stability of the anionic species is significantly affected by the electronic structure, where the [5,6]-double bond is responsible for the instability of the reduced species of the para adducts. Further study with 1,15-$(MeO)_2$-2,4-Bn_2C_{60}, an adduct with both the ortho and para positioned methoxy, shows that the reduced species is stable, indicating that the 1,2,4,15-configuration is an electronically preferential structure even though it has a [5,6]-double bond.

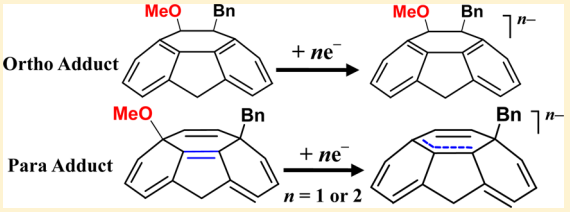

INTRODUCTION

The electronic and steric effects are the two most important factors that influence the reactivity and structure of organic molecules. For fullerene derivatives,[1,2] the electronically favored products are the ortho adducts, as all the double bonds are positioned between the two hexagons, retaining the electronic structure of pristine fullerenes. While the sterically favored ones are the para adducts, in which an electronically unfavored [5,6]-double bond is introduced,[3] but this increased energy can be compensated for by a decrease in steric hindrance when bulky addends are involved. The effects of the electronic and steric factors on the stabilization of neutral organic molecules have been well studied. However, much less is known regarding these effects toward the stabilization of charged molecules, likely due to the difficulty in obtaining both the electronically and sterically favored regioisomers that are also of electrochemical activity. Organofullerenes are ideal model molecules for such study. First, it is possible to obtain both the ortho and para fullerene adducts, even though the amount of one regioisomer may be very small.[4] Second, the fullerene derivatives are typically of electrochemical activity, rendering them suitable for the study of anionic species.[5]

Although the steric factor plays an important role in formation of neutral fullerene para adducts, the preliminary result on sterically favored C_{60} imidazoline derivatives indicates that such a factor has little effect in stabilizing the anionic species compared with the electronic factor,[6] suggesting an important difference between the steric and electronic factors. Herein, we report the stability examination of the anionic species of organofullerenes **1**−**5** (Scheme 1), which shows a distinct difference between the ortho and para adducts and may help to obtain a better understanding on the electronic vs steric effects toward the stabilization of anionic species.

RESULTS AND DISCUSSION

Preparation of Compounds 1−5. Compounds **1**, **2**, and **5** were prepared by the reaction of C_{60} with MeO^- and BnBr following procedures reported previously, and the identity of each compound was confirmed with spectroscopic characterizations by comparing with the reported data.[7] Compounds **3** and **4** were synthesized with procedures similar to those for preparing **1** and **2**, except C_{70} was used instead of C_{60}. Under typical conditions, the yield for **3** and **4** is 34.1% and 2.9%, respectively.

The structures of **3** and **4** were established on the basis of X-ray single-crystal diffraction, HRMS, ^{1}H and ^{13}C NMR, and UV−vis spectroscopic characterizations. Figure 1 displays the X-ray single-crystal structure of **3**, which was obtained by slowly diffusing n-hexane into the CS_2 solution of **3** at room temperature. The structure shows unambiguously that compound **3** is an ortho adduct, with the methoxy group positioned at C2 and the benzyl bonded to C1 of C_{70} cage (1-Bn-2-MeOC_{70}). In principle, there should be another 1,2-adduct, 1-MeO-2-BnC_{70}, with the locations of the benzyl and methoxy groups switched with respect to those in **3** due to the low symmetry of C_{70}, as reported for other C_{70} derivatives.[9] However, no such compound is found from the reaction, indicating that the reaction proceeds via a rather regioselective manner. The result is consistent with the high regioselectivity exhibited by the reactions of anionic oxygen nucleophiles with less symmetrical C_{60} derivatives,[7,10] suggesting that the formation of **3** is likely initiated by the nucleophilic addition of MeO^- to C_{70} at C2, as C2 is the most reactive carbon atom in C_{70} due to the largest strain it experiences.[11]

Received: October 29, 2014
Published: December 29, 2014

DOI: 10.1021/jo502475w
J. Org. Chem. 2015, 80, 1557−1563

Scheme 1. Structures of Compounds 1–5[8]

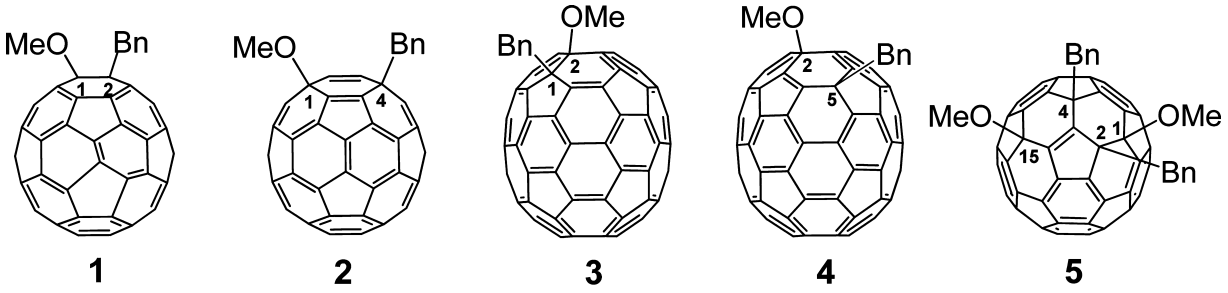

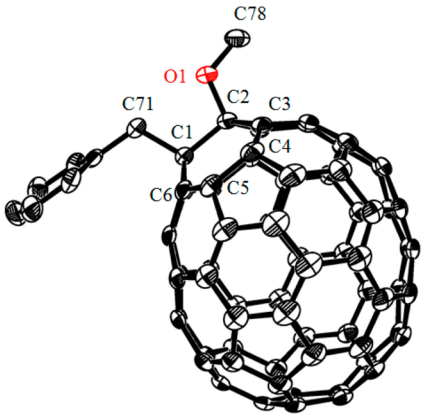

Figure 1. ORTEP diagram for **3** with 30% thermal ellipsoids. Hydrogen atoms are omitted for clarity. Selected bond distances (Å): C1–C2, 1.602; C2–C3, 1.543; C3–C4, 1.376; C4–C5, 1.460; C5–C6, 1.357; C6–C1, 1.526; C2–O1, 1.445; C78–O1, 1.423; C1–C71, 1.589. Selected bond angles (deg): C1–C2–C3, 113.8; C2–C3–C4, 123.2; C3–C4–C5, 121.3; C4–C5–C6, 120.0; C5–C6–C1, 124.8; C6–C1–C2, 114.3.

The structure of compound **3** is further supported by the spectroscopic characterizations. HRMS of the compound (Figure S3, Supporting Information) shows the molecular ion at 962.0719, consistent with the structure of 1,2-Bn(MeO)C_{70} (calcd m/z 962.0732). The UV–vis spectrum of the compound (Figure S4, Supporting Information) shows absorption bands at 341, 396, 460, 533, and 657 nm, which are essentially identical to the absorption patterns of 1,2-C_{70} adducts,[9b,c,12] except a slight shift of a few nanometers in wavelength likely caused by the variance of the addends. The ^{1}H NMR spectrum (Figure S5, Supporting Information) shows two singlet resonances at 4.43 and 4.00 ppm corresponding to the methoxy and methylene protons, respectively, and the ^{13}C NMR spectrum (Figure S6, Supporting Information) shows 30 signals for the sp^2 C_{70} carbons, consistent with the C_S symmetry of the compound.

As for compound **4**, the HRMS spectrum (Figure S7, Supporting Information) shows the molecular ion at 962.0749, suggesting that it also has the formula of (MeO)BnC_{70} (calcd m/z 962.0732). Absorption bands characteristic of the 2,5-C_{70} adducts are displayed at 360, 417, 591, and 706 nm,[13] indicating that the compound is a 2,5-adduct. A singlet resonance at 3.80 ppm for the methoxy protons and an AB quartet at 3.29 and 3.21 ppm for the diastereotopic methylene protons of the benzyl appear in the ^{1}H NMR spectrum (Figure S9, Supporting Information), which provides the key evidence regarding the configuration of the compound. Previous work on 2,5-Bn_2C_{70} has shown that the diastereotopic methylene protons of a C2-bound benzyl resonate at 3.60 ppm as a singlet, due to the less restricted rotation of the phenyl ring. On the contrary, the counterparts of a C5-bound benzyl resonate at 3.22 and 3.19 ppm as an AB quartet, because of the more confined rotation of the phenyl ring.[13b] This result indicates explicitly that the benzyl group in compound **4** is bound to C5, and that the methoxy group is located at C2. The ^{13}C NMR spectrum of compound **4** (Figure S10, Supporting Information) shows a total of 64 sp^2 C_{70} carbon signals, along with resonances for the two sp^3 C_{70} (80.43 and 55.81 ppm) and benzyl carbon atoms, consistent with the C_1 symmetry of the molecule. The bonding of the methoxy group at the C2 atom in both **3** and **4** indicates that the two compounds are likely formed via the same intermediate, 2-MeOC_{70}^-, followed by the electrophilic addition of the benzyl with either the ortho or the para manner, consistent with the mechanism for formation of C_{60} analogues **1** and **2**.[7]

Electrochemical Study of Compounds 1–4. Figure 2 shows the cyclic voltammograms (CVs) of compounds **1** and **2** recorded in PhCN solution containing 0.1 M tetra-*n*-butylammonium perchlorate (TBAP) as the electrolyte, with a saturated calomel electrode (SCE) as the reference electrode.

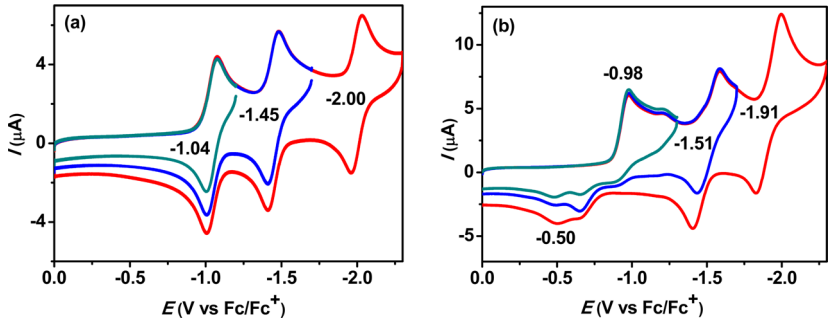

Figure 2. Cyclic voltammograms of compounds (a) **1** and (b) **2** in PhCN containing 0.1 M TBAP. Scan rate = 100 mV/s.

DOI: 10.1021/jo502475w
J. Org. Chem. 2015, 80, 1557–1563

Compound **1** exhibits three quasireversible one-electron transfer processes with $E_{1/2}$ at −1.04, −1.45, and −2.00 V vs ferrocene/ferrocenium (Fc/Fc^+, the $E_{1/2}$ for the Fc/Fc^+ redox couple is measured to be at 0.50 V vs SCE under experimental conditions, Figure S11, Supporting Information), indicating that the anionic species of **1** are stable. The result is typical for fullerene derivatives in view of both the reversibility and redox potentials,[5] where the potentials are cathodically shifted with respect to those of C_{60} due to the cleavage of the π-conjugation.

However, a completely different scenario is shown for the CV of compound **2** (Figure 1b). The first redox wave shows an irreversibility nature with E_{pc} at −0.98 V vs Fc/Fc^+ and a broad oxidation wave ranging from about −0.90 to −0.48 V vs Fc/Fc^+, indicating that a chemical process likely occurs as the compound acquires one electron. Further reduction of the compound results in two quasireversible redox waves with $E_{1/2}$ at −1.51 and −1.91 V, and an irreversible oxidation wave around −0.50 V, which are comparable to the redox processes involving the singly bonded C_{60} and dimeric species,[14,15] suggesting that compound **2** undergoes a reductive decomposition.

Controlled-potential bulk electrolyses (CPE) of **1** and **2** were performed to further probe the property of the singly reduced **1** and **2**. The monoanions of **1** and **2** were generated with CPE by applying a potential at −1.30 V vs Fc/Fc^+, and a transfer of only one electron per mole molecule was strictly controlled. The vis-NIR spectrum of the singly reduced **1** (Figure 3) shows

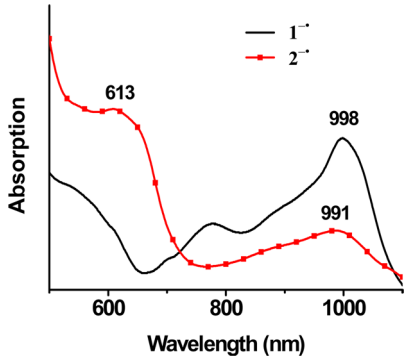

Figure 3. Vis-NIR spectra of the in situ-generated singly reduced species of compounds **1** and **2** in PhCN solution containing 0.1 M TBAP.

a major absorption band at 998 nm, which is characteristic of the monoanions of 1,2-adducts of C_{60},[4b,16] consistent with the cyclic voltammetry result that the monoanion of **1** is stable. As for the singly reduced **2**, the spectrum (Figure 3) shows one absorption band at 991 nm and an intense band at 613 nm, which is the diagnostic band for the monoanionic species of singly bonded C_{60} (RC_{60}^-),[7,17] indicating that a reductive decomposition reaction indeed occurs. Notably, the absorption band at 991 nm is rather broad, indicating the likely presence of a mixture in the solution of singly reduced **2**.

The singly reduced **1** and **2** were oxidized back to neutral by CPE with a potential set at 0 V vs Fc/Fc^+, and the obtained products were subjected to the HPLC analysis. The results show that compound **1** is completely recovered after the reduction and oxidation cycle, with no decomposition (Figure S12, Supporting Information, for HPLC trace). While the HPLC trace of the oxidation products of $\mathbf{2}^-$ (Figure 4) shows two major fractions with retention time at 6.3 and 9.9 min,

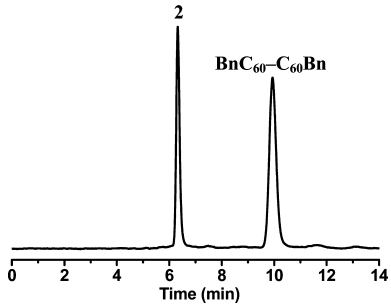

Figure 4. HPLC trace of the reaction mixture obtained by electrooxidation of the singly reduced **2**. The mixture was eluted with toluene over a Buckyprep column with a flow rate of 3.7 mL/min. The detector wavelength was set at 380 nm.

which are ascribed to compound **2** and $BnC_{60}–C_{60}Bn$, respectively. The formation of $BnC_{60}–C_{60}Bn$ is verified by the ^1H NMR and UV–vis spectral characterizations as compared with previous work,[14] indicating that the methoxy group is the one being cleaved from **2** upon reduction. The recovery of a significant amount of **2** in the HPLC trace indicates that both $\mathbf{2}^-$ and BnC_{60}^- are present in the solution of singly reduced **2**, suggesting that the decomposition of $\mathbf{2}^-$ is likely a slow process, consistent with the broad nature of the absorption band in the vis-NIR spectrum of $\mathbf{2}^-$.

To the best of our knowledge, this is the first time that a stability difference has been shown between the anionic species of the ortho and para regioisomers of C_{60} adducts. Previous work on C_{60} derivatives with alkyl or aryl addends has shown that the anions of both regioisomers are stable, with a difference only in the redox potentials,[4b,18] indicating that the presence of a good leaving group, the methoxy group, is crucial in identifying the stability difference between the reduced isomeric species. Because the ortho and para fullerene adducts are formed due to the electronic and steric factors, respectively, the result may provide insights into the electronic vs steric effects on the stability of anionic species.

Further study was carried out on the ortho and para regioisomers of $(MeO)BnC_{70}$ (**3** and **4**). Figure 5 shows the CVs of compounds **3** and **4** recorded in PhCN containing 0.1 M TBAP. Similar to **1**, the analogue of the C_{60} derivative, compound **3** is electrochemical stable and exhibits three quasireversible one-electron transfer processes with $E_{1/2}$ at −1.05, −1.43, and −1.84 V vs Fc/Fc^+ within the electrochemical window (Figure 5a), consistent with the results of typical fullerene derivatives in view of redox potentials and reversibility.[5]

In contrast, compound **4**, the para adduct, is electrochemically unstable by showing two closely positioned redox waves ($E_{1/2}$: −1.24 and −1.42 V vs Fc/Fc^+) in the cyclic voltammogram (Figure 5b). Under typical conditions, the redox waves of fullerenes and their derivatives are well separated by about 400–600 mV.[5] The redox waves with $E_{1/2}$ at −0.83, −1.24, and −1.83 V vs Fc/Fc^+ for compound **4** are in good agreement with such separations. However, the waves at −1.24 and −1.42 V are much less parted from each other with a difference of only 180 mV, suggesting that these two redox processes likely originate from different fullerene species. In addition, as the compound is further reduced, new anodic waves with E_{pa} at around −0.48 V appear, which are related to the formation of singly bonded fullerene dimers as shown previously,[14,15] suggesting that the methoxy group is likely

DOI: 10.1021/jo502475w
J. Org. Chem. 2015, 80, 1557–1563

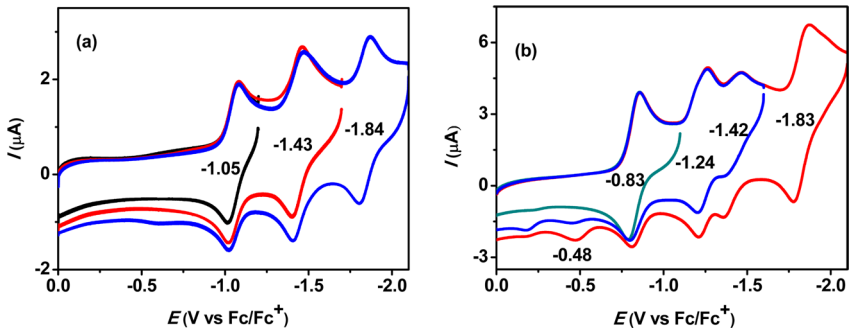

Figure 5. Cyclic voltammograms of compounds (a) **3** and (b) **4** in PhCN containing 0.1 M TBAP with a scan rate of 100 mV/s.

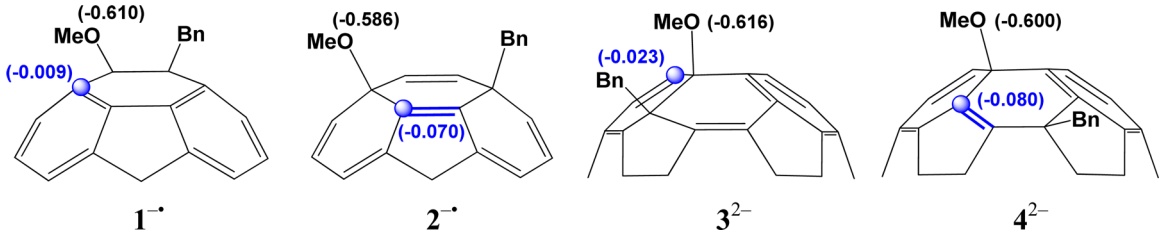

Figure 6. Calculated NBO charges at the oxygen atom of the methoxy group and one of the neighboring sp^2 carbon atoms that bears the largest charge in $\mathbf{1}^{\bullet-}$, $\mathbf{2}^{\bullet-}$, $\mathbf{3}^{2-}$, and $\mathbf{4}^{2-}$.

removed after compound **4** is reduced, similar to the reductive decomposition of compound **2**.

The result demonstrates explicitly that the anionic species of the para adducts of C_{60} and C_{70} are unstable, while the ortho ones are stable. The availability of **1**−**4** indicates that both the ortho and para adducts of C_{60} and C_{70} are stable in the neutral form as a result of the electronic and steric factors. However, the steric factor, which has played a key role in constituting the neutral para adducts, seems to have no effect in stabilizing the anionic structure of the compounds. Instead, the electronic factor, which accounts for the stability of the neutral ortho adducts, seems to be still capable of stabilizing the compounds in anionic forms.

Mechanistic Consideration on the Stability Difference between the Anionic Species of 1−4. Computational calculations were carried out on the anionic species of **1**−**4** in order to identify the factor that is responsible for the stability difference between the anionic species of the two types of regioisomers. As the methoxy group is the one being cleaved during the reduction process, the attention is paid to the methoxy group and the vicinal fullerene carbon atoms. Figure 6 illustrates the NBO charges at the oxygen atom of the methoxy group and one of the neighboring sp^2 carbon atoms that bears the largest charge in $\mathbf{1}^{\bullet-}$, $\mathbf{2}^{\bullet-}$, $\mathbf{3}^{2-}$, and $\mathbf{4}^{2-}$, calculated with Gaussian 09 program at B3LYP/6-311G(d)//B3LYP/6-31G level (see Figures S13−S16, Supporting Information, for more charge distributions).

The calculations predict a similar negative charge at the oxygen atom in $\mathbf{1}^{\bullet-}$ (−0.610), $\mathbf{2}^{\bullet-}$ (−0.586), $\mathbf{3}^{2-}$ (−0.616), and $\mathbf{4}^{2-}$ (−0.600), with the ortho adducts bearing a slightly greater charge compared with the para ones, suggesting that the reductive removal of the methoxy group in the para regioisomers is unlikely related to the charge distribution at the oxygen atom. Instead, a much significant difference is predicted for the charge localized at the sp^2 carbon atom adjacent to the C_{2n}−OMe bond between the ortho and para regioisomers. The greatest charge among the sp^2 carbon atoms next to the C_{60}−OMe bond is only −0.009 in $\mathbf{1}^{\bullet-}$ (ortho adduct), while a much larger amount of charge of −0.070 is predicted at the sp^2 carbon atom adjacent to the C_{60}−OMe bond in $\mathbf{2}^{\bullet-}$ (para adduct), which is also the carbon atom constituting the [5,6]-double bond. Similarly, the same trend is observed in the C_{70} analogues, where the sp^2 carbon atom next to the C_{70}−OMe bond in $\mathbf{3}^{2-}$ (ortho adduct) bears a small amount of charge (−0.023), while the counterpart in $\mathbf{4}^{2-}$ (para adduct) bears a large amount of charge (−0.080).

The accumulation of a large amount of charge at the [5,6]-double bond in $\mathbf{2}^{\bullet-}$ and $\mathbf{4}^{2-}$ is consistent with previous work that the LUMO is localized at the [5,6]-double bond in the neutral C_{60} para adducts[18,19] and it may subsequently induce the reductive cleavage of the methoxy group as illustrated in Figure 7. The distinct [5,6]-double bond nature in $\mathbf{2}^{\bullet-}$ is

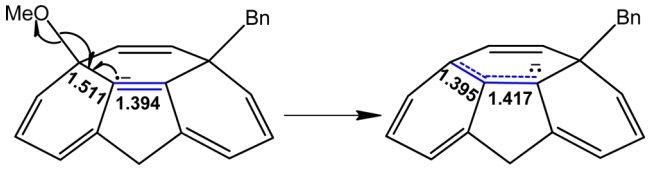

Figure 7. Illustration of the charge-induced reductive cleavage of the methoxy group from $\mathbf{2}^{\bullet-}$. The numbers indicate the selected bond length (Å) for the optimized 1,4-(MeO)$BnC_{60}^{\bullet-}$ and BnC_{60}^{-} calculated at the HF/6-31G level.

blurred in BnC_{60}^{-} after removing the methoxy group, as the bond length is predicted to be elongated from 1.394 to 1.417 Å (Gaussian 09 at HF/6-31G level). Meanwhile, the single [6,6]-bond in $\mathbf{2}^{\bullet-}$ would possess a significant double bond nature in BnC_{60}^{-}, as the bond length is predicted to be shortened from 1.511 to 1.395 Å by calculations at the same level. A stable allyl anion is therefore formed with the largest negative charge located at the ortho and para carbon atoms with respect to the singly bonded benzyl group, indicating that the driving force for the reductive decomposition of the para adducts is to restore the electronic structure back to that of pristine fullerenes by eliminating the [5,6]-double bond. The results show that the

DOI: 10.1021/jo502475w
J. Org. Chem. 2015, 80, 1557−1563

unfavored electronic structure of the para adducts is responsible for the reductive decomposition, indicating that different from neutral compounds, where both the electronic and steric factors are important for the stability, only the electronic factor is important in affecting the stability of the anionic species, while the steric factor has no effect.

In addition, the anionic species of C_{70} para adduct (**4**) exhibits a stability better than that of the C_{60} counterpart (**2**) as indicated by the CV measurement, as it requires the addition of two electrons to initiate the reductive decomposition of **4**. The extra stability for $\mathbf{4}^{\bullet-}$ is likely related to the unique bond delocalization in the equatorial region of C_{70} cage,[20] which may construct a cyclopentadiene structure with the [5,6]-double bond in the polar region to delocalize the acquired charge.[21] Figure 8 shows the partial structures with bond labeling for $\mathbf{2}^{\bullet-}$

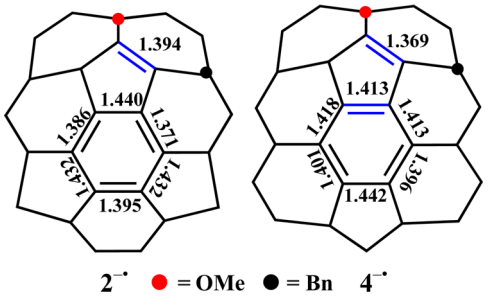

Figure 8. Partial structures with bond length labeling for $\mathbf{2}^{\bullet-}$ and $\mathbf{4}^{\bullet-}$ calculated at the HF/6-31G level.

and $\mathbf{4}^{\bullet-}$ calculated at the HF/6-31G level. A cyclopentadiene structure is predicted in $\mathbf{4}^{\bullet-}$, as the [5,6]-bond in the equatorial region exhibits a strong double bond nature by having a bond length of 1.413 Å, while no such unit is predicted in $\mathbf{2}^{\bullet-}$, where all the other double bonds are located at the [6,6]-bonds, making the structure rather unstable after receiving one electron.

Further Study with 1,15-(MeO)$_2$-2,4-Bn$_2$C$_{60}$. Compound **5** (1,15-(MeO)$_2$-2,4-Bn$_2$C$_{60}$) is an interesting adduct for further study, as it contains both the ortho- and para-positioned methoxy groups.[7] Figure 9 shows the CV of compound **5**.

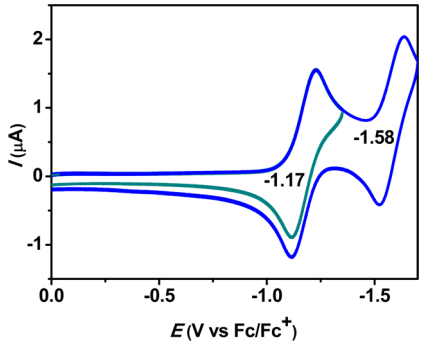

Figure 9. Cyclic voltammogram of compound **5** in PhCN containing 0.1 M TBAP. Scan rate = 100 mV/s.

Surprisingly, the CV displays two quasireversible redox processes with $E_{1/2}$ at −1.17 and −1.58 V vs Fc/Fc$^+$, demonstrating that the singly and doubly reduced species of **5** are stable, with no charge-induced reductive removal of the methoxy group occurring, even though the compound has a para-positioned methoxy group.

Figure 10 shows the calculated NBO charge at the [5,6]-double bond carbon atom adjacent to the C_{60}−OMe bond in

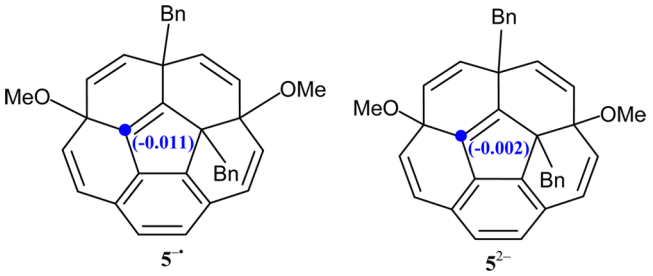

Figure 10. NBO charges at the [5,6]-double bond carbon atoms next to the C_{2n}−OMe bond in $\mathbf{5}^{\bullet-}$ and $\mathbf{5}^{2-}$.

$\mathbf{5}^{\bullet-}$ and $\mathbf{5}^{2-}$ (B3LYP/6-311G(d)//B3LYP/6-31G; see Figures S17 and S18, Supporting Information, for more NBO charge distributions). Different from $\mathbf{2}^{\bullet-}$ and $\mathbf{4}^{2-}$, the calculations predict a much less amount of charge at the [5,6]-double bond in $\mathbf{5}^{\bullet-}$ (−0.011) and $\mathbf{5}^{2-}$ (−0.002), suggesting that there is no significant charge buildup at the [5,6]-double bond in the singly and doubly reduced species of **5**, and the charge-induced cleavage of the methoxy group would be therefore unlikely. It indicates that the 1,2,4,15-configuration for C_{60} adducts is an electronically preferential one, where the para addition manner in the derivatives should be due to the electronic factor, rather than the steric factor. The result is consistent with the fact that the 1,2,4,15-configuration is so far the most encountered structure for C_{60} derivatives containing both the 1,2- and 1,4-addition patterns,[7,22] whose formation is proposed to involve an electronically preferential 10π $R_3C_{60}^-$ indenyl anion intermediate with three para-positioned addends.[22b,c]

CONCLUSION

With the use of ortho and para regioisomers of (MeO)BnC$_{60}$ (**1** and **2**) and (MeO)BnC$_{70}$ (**3** and **4**) as model compounds, the effects of the electronic and steric factors toward the stabilization of reduced species have been studied. The ortho adducts are stable upon receiving one and two electrons, while the para adducts undergo reductive decomposition under similar conditions by removing the methoxyl group. Computational calculations indicate that the electronically unfavored [5,6]-double bond is responsible for the structure instability of the para adducts, driven by the force to restore the disadvantageous electronic structure back to the preferential one. The work has shown that different from the situation for neutral compounds, where both the electronic and steric effects are important for the stability of the compounds, only the electronic factor is important in determining the stability of the anionic species, while the steric factor has no effect.

EXPERIMENTAL SECTION

General Methods. Compounds **1**, **2**, and **5** were synthesized according to our previously reported procedure.[7] All the CVs and electrochemical reactions were performed under Ar atmosphere. Electrochemical grade TBAP was recrystallized from absolute ethanol and dried in a vacuum at 298 K prior to use. PhCN was distilled over P_2O_5 under vacuum at 305 K prior to use. All other chemicals were commercially available and used as received. Controlled-potential bulk electrolysis was carried out on a potentiostat/galvanostat using an "H" type cell which consisted of two platinum gauze electrodes (working and counter electrodes) separated by a sintered glass frit. A conventional three-electrode cell was used for CV measurements

DOI: 10.1021/jo502475w
J. Org. Chem. 2015, 80, 1557−1563

and consisted of a glassy carbon working electrode, a platinum counter electrode, and a SCE reference electrode. The SCE was separated from the bulk of the solution by a fritted-glass bridge of low porosity, which contained the solvent/supporting electrolyte mixture.

Synthesis of Compounds 3 and 4. Typically, 42 mg of C_{70} (50 μmol) and BnBr (120 μL, 0.10 mmol) were added into 20 mL of ODCB (*o*-dichlorobenzene) solution degassed with argon at 120 °C. Then 8 equiv of TBAOH (1.0 M in methanol, 400 μL) was added into the solution, and the reaction was allowed to proceed for 2 h. The reaction mixture was dried with a rotary evaporator, and the residue was washed with methanol to remove excess TBAOH and BnBr. The crude product was eluted with toluene over a semipreparative Buckyprep column (10 mm × 250 mm) at a flow rate of 3.7 mL/min with the detector wavelength set at 380 nm, which afforded a mixture of **3** and **4** and 12.7 mg of unreacted C_{70} (30.3%). The mixture of **3** and **4** was further purified by eluting with 70:30 v/v toluene/hexane mixture over a semipreparative silica column, and it afforded 16.4 mg of **3** (34.1%) and 1.4 mg of **4** (2.9%) respectively.

Spectral Characterization of 3. Negative ESI-ICR MS: calcd for M^- ($C_{78}H_{10}O^-$) 962.0732, found 962.0719; ^{1}H NMR (600 MHz, CS_2/$CDCl_3$) δ 7.18−7.03 (m, 5H), 4.37 (s, 3H), 3.93(s, 2H); ^{13}C NMR (150 MHz, CS_2/ $CDCl_3$) δ 164.13 (2C), 154.35 (2C), 151.03 (2C), 150.82 (4C), 150.78 (4C), 150.34 (2C), 149.35 (2C), 149.10 (2C), 149.06 (2C), 148.75 (4C), 148.57(2C), 147.23 (2C), 147.74 (1C), 147.04 (4C), 146.93 (2C), 146.35 (2C), 146.21 (2C), 145.63 (2C), 145.03 (1C), 143.45 (2C), 143.23 (4C), 142.37 (2C), 141.13 (2C), 140.47 (2C), 137.91 (2C), 136.44 (2C), 133.60 (2C), 131.42 (2C, Ph), 131.24 (2C), 131.05 (2C), 130.90 (2C), 127.62 (2C, Ph), 126.63 (2C, Ph), 91.47 (1C, sp^3, C_{70}−O), 61.88 (1C, sp^3, C_{70}−CH_2), 55.87 (1C, sp^3,O−CH_3), 40.33(1C, sp^3, CH_2) ; UV−vis (toluene) λ_{max}: 341, 396, 460, 533, and 657 nm.

X-ray Crystallographic Data Collection and Structure Refinement. Black lamellar crystals of compound **3** suitable for an X-ray analysis were obtained by slowly diffusing hexane into a CS_2 solution of compound **3** at room temperature. Single-crystal X-ray diffraction data were collected on an instrument equipped with a CCD area detector using graphite-monochromated Mo Kα radiation (λ = 0.71073 Å) in the scan range 1.54° < θ < 26.07°. The structure was solved with the direct methods using SHELXS-97 and refined with full-matrix least-squares techniques using the SHELXL-97 program within WINGX. X-ray Crystal data for **3**: Empirical formula: $C_{78}H_{10}O$; formula weight: 962.86; crystal system, space group: monoclinic, P2(1)/c; unit cell dimensions: a = 10.9318 Å, b = 17.8483 Å, c = 20.0007 Å, α = 90.00°, β = 102.88°, γ = 90.00°; V: 3804.2(5) Å^3; calculated density: 1.681 g cm^{-3}; crystal size: 0.33 × 0.28 × 0.18 mm; reflections collected: 22318; max. and min transmission: 0.9825 and 0.9683; final R indices [$I > 2\sigma(I)$]: R_1 = 0.0516, wR_2 = 0.0986; R indices (all data): R_1 = 0.0774, wR_2 = 0.1097.

Spectral Characterization of 4. Negative ESI-ICR MS: calcd for M^- ($C_{78}H_{10}O^-$) 962.0732, found 962.0749; ^{1}H NMR (400 MHz, with d_6-DMSO as the external lock solvent) δ 6.96 (t, 3H), 6.87 (m, 2H), 3.80 (s, 3H); 3.24, 3.18 (AB_q, J = 13 Hz, 2H); ^{13}C NMR (125 MHz, in CS_2 with DMSO-d_6 as the external lock solvent, all 1 C unless indicated) 169.05, 164.51, 161.83, 153.04, 158.87, 151.64, 151.58, 150.11, 149.75, 149.66, 149.54, 149.43, 149.41, 149.17, 149.10, 149.04, 148.17, 148.12, 147.98, 147.82, 147.73, 147.56, 147.49, 147.48, 147.44, 147.39, 147.28, 146.81, 146.43, 146.16, 145.92 (2C), 145.90, 145.90, 145.86, 145.47, 145.24, 145.05, 144.94, 144.82, 144.60, 144.46, 144.33, 143.79, 143.44, 143.33, 142.90, 142.74, 142.68, 142.61, 142.55, 142.37, 147.70, 140.77, 136.50, 135.49 (2C), 135.30, 135.22, 132.71, 132.64, 132.60, 132.44, 132.19, 130.84, 130.48, 130.12 (2C, Ph), 129.46, 129.09, 128.68, 128.07 (2C, Ph), 127.26 (2C, Ph), 80.43 (1C, sp^3, C_{60}−OCH_3), 55.79 (1C, sp^3, C_{60}−CH_2), 55.06 (1C, sp^3,O−CH_3), 43.32 (1C, sp^3, CH_2); UV−vis (toluene) λ_{max}: 360, 417, 591, 706 nm.

Visible and Near-IR Measurements of Monoanions of 1 and 2. The monoanions of **1** and **2** were generated electrochemically by applying a reducing potential at −0.8 V vs SCE (−1.30 vs Fc/Fc^+), and a transfer of only one electron per mole molecule was strictly controlled. Typically, the CPE was carried out using an amount of about 12 mg of the sample in 20 mL of 0.1 M TBAP PhCN solution under argon. The generated anionic species were transferred into an airtight 1 cm quartz cuvette under deaerated condition. The near-IR spectrum of the monoanions of **1** and **2** were measured under argon at room temperature.

Computational Methods. The structures of $\mathbf{1}^{\bullet-}$, $\mathbf{2}^{\bullet-}$, $\mathbf{3}^{2-}$, $\mathbf{4}^{2-}$, $\mathbf{5}^{\bullet-}$, and $\mathbf{5}^{2-}$ were optimized with Gaussian 09 at the DFT/B3LYP level using the 6-31G basis set, followed by harmonic frequency calculations at the same level to confirm them as the energy minima. The NBO charge distribution calculations of $\mathbf{1}^{\bullet-}$, $\mathbf{2}^{\bullet-}$, $\mathbf{3}^{2-}$, $\mathbf{4}^{2-}$, $\mathbf{5}^{\bullet-}$, and $\mathbf{5}^{2-}$ were performed at the B3LYP/6-311G(d) level on the basis of the optimized structures (B3LYP/6-31G). The structures of $\mathbf{2}^{\bullet-}$, BnC_{60}^-, and $\mathbf{4}^{\bullet-}$ with all real frequencies were obtained with Gaussian 09 at the Hartree−Fock (HF) level with the 6-31G basis set.

■ ASSOCIATED CONTENT

Supporting Information

X-ray CIF file of compound **3**, HPLC traces of the reaction mixtures, spectral data of new compounds, and computational details. This material is available free of charge via the Internet at http://pubs.acs.org.

■ AUTHOR INFORMATION

Corresponding Author

*E-mail: xgao@ciac.ac.cn.

Notes

The authors declare no competing financial interest.

■ ACKNOWLEDGMENTS

The work was supported by the National Natural Science Foundation of China (21172212 and 21472183 for X.G. and 21202157 for Z.J.L.).

■ REFERENCES

(1) Hirsch, A.; Brettreich, M. *Fullerenes: Chemistry and Reactions*; Wiley-VCH, Weinheim, Germany, 2005.

(2) Diederich, F.; Thilgen, C. *Science* **1996**, *271*, 317−323.

(3) Matsuzawa, N.; Dixon, D. A.; Fukunaga, T. *J. Phys. Chem.* **1992**, *96*, 7594−7604.

(4) (a) Allard, E.; Delaunay, J.; Cheng, F.; Cousseau, J.; Ordúna, J.; Garín, J. *Org. Lett.* **2001**, *3*, 3503−3506. (b) Zheng, M.; Li, F.; Shi, Z.; Gao, X.; Kadish, K. M. *J. Org. Chem.* **2007**, *72*, 2538−2542.

(5) Echegoyen, L.; Echegoyen, L. E. *Acc. Chem. Res.* **1998**, *31*, 593−601.

(6) Hou, H.-L.; Li, Z.-J.; Gao, X. *Org. Lett.* **2014**, *16*, 712−715.

(7) Chang, W.-W.; Li, Z.-J.; Yang, W.-W.; Gao, X. *Org. Lett.* **2012**, *14*, 2386−2389.

(8) For numbering of C_{60} and C_{70}, see: Godly, E. W. T. R. *Pure Appl. Chem.* **1997**, *69*, 1411−1134.

(9) (a) Meier, M. S.; Poplawska, M.; Compton, A. L.; Shaw, J. P.; Selegue, J. P.; Guard, T. F. *J. Am. Chem. Soc.* **1994**, *116*, 7044−7048. (b) Wang, Z.; Meier, M. S. *J. Org. Chem.* **2003**, *68*, 3043−3048. (c) Ni, L.; Chang, W.; Hou, H.-L.; Li, Z.-J.; Gao, X. *Org. Biomol. Chem.* **2011**, *9*, 6646−6653.

(10) Li, Z.-J.; Li, F.-F.; Li, S.-H.; Chang, W.-W.; Yang, W.-W.; Gao, X. *Org. Lett.* **2012**, *14*, 3482−3485.

(11) Thilgen, C.; Diederich, F. *Top. Curr. Chem.* **1999**, *199*, 135−171.

(12) (a) Henderson, C. C.; Rohifing, C. M.; Gillen, K. T.; Cahill, P. A. *Science* **1994**, *264*, 397−399. (b) Meier, M. S.; Bergosh, R. G.; Gallagher, M. E.; Spielmann, H. P.; Wang, Z. *J. Org. Chem.* **2002**, *67*, 5946−5952.

(13) (a) Popov, A. A.; Kareev, I. E.; Shustova, N. B.; Lebedkin, S. F.; Strauss, Steven H.; Boltalina, O. V.; Dunsch, L. *Chem.—Eur. J.* **2008**, *14*, 107−121. (b) Li, S.-H.; Li, Z.-J.; Yang, W.-W.; Gao, X. *J. Org. Chem.* **2013**, *78*, 7208−7215.

(14) Yang, W.-W.; Li, Z.-J.; Gao, X. *J. Org. Chem.* **2011**, *76*, 6067−6074.

DOI: 10.1021/jo502475w
J. Org. Chem. 2015, 80, 1557−1563

(15) (a) Cheng, F.; Murata, Y.; Komatsu, K. *Org. Lett.* **2002**, *4*, 2541−2544. (b) Ocafrain, M.; Herranz, M. A.; Marx, L.; Thilgen, C.; Diederich, F.; Echegoyen, L. *Chem.−Eur. J.* **2003**, *9*, 4811−4819.
(16) Kadish, K. M.; Gao, X.; Van Caemelbecke, E.; Suenobu, T.; Fukuzumi, S. *J. Phys. Chem. A* **2000**, *104*, 3878−3883.
(17) (a) Kitagawa, T.; Tanaka, T.; Tanaka, Y.; Takeuchi, K.; Komatsu, K. *J. Org. Chem.* **1995**, *60*, 1490−1491. (b) Tanaka, T.; Kitagawa, T.; Komatsu, K.; Takeuchi, K. *J. Am. Chem. Soc.* **1997**, *119*, 9313−9314. (c) Fukuzumi, S.; Suenobu, T.; Hirasaka, T.; Arakawa, R.; Kadish, K. M. *J. Am. Chem. Soc.* **1998**, *120*, 9220−9227.
(18) Popov, A. A.; Kareev, I. E.; Shustova, N. B.; Stukalin, E. B.; Lebedkin, S. F.; Seppelt, K.; Strauss, S. H.; Boltalina, O. V.; Dunsch, L. *J. Am. Chem. Soc.* **2007**, *129*, 11551−11568.
(19) Popov, A. A.; Kareev, I. E.; Shustova, N. B.; Strauss, S. H.; Boltalina, O. V.; Dunsch, L. *J. Am. Chem. Soc.* **2010**, *132*, 11709−11721.
(20) Meier, M. S.; Wang, G.-W.; Haddon, R. C.; Brock, C. P.; Lloyd, M. A.; Selegue, J. P. *J. Am. Chem. Soc.* **1998**, *120*, 2337−2342.
(21) (a) Akasaka, T.; Suzuki, T.; Maeda, Y.; Ara, M.; Wakahara, T.; Kobayashi, K.; Nagase, S.; Kako, M.; Nakadaira, Y.; Fujitsuka, M.; Ito, O. *J. Org. Chem.* **1998**, *64*, 566−569. (b) Hou, H.-L.; Li, Z.-J.; Wang, Y.; Gao, X. *J. Org. Chem.* **2014**, *79*, 8865−8870.
(22) (a) Kadish, K. M.; Gao, X.; Van Caemelbecke, E.; Suenobu, T.; Fukuzumi, S. *J. Am. Chem. Soc.* **2000**, *122*, 563−570. (b) Sawamura, M.; Toganoh, M.; Suzuki, K.; Hirai, A.; Iikura, H.; Nakamura, E. *Org. Lett.* **2000**, *2*, 1919−1921. (c) Toganoh, M.; Suzuki, K.; Udagawa, R.; Hirai, A.; Sawamura, M.; Nakamura, E. *Org. Biomol. Chem.* **2003**, *1*, 2604−2611. (d) Nambo, M.; Wakamiya, A.; Yamaguchi, S.; Itami, K. *J. Am. Chem. Soc.* **2009**, *131*, 15112−15113.

DOI: 10.1021/jo502475w
J. Org. Chem. 2015, 80, 1557−1563